HHS Public Access

Author manuscript

Laryngoscope. Author manuscript; available in PMC 2019 February 01.

Published in final edited form as:

Laryngoscope. 2018 February ; 128(2): E59–E67. doi:10.1002/lary.26893.

Targeting Metabolic Abnormalities to Reverse Fibrosis in Iatrogenic Laryngotracheal Stenosis

Michael K. Murphy, MD, **Kevin M Motz, MD**, **Dacheng Ding, MD, PhD**, **Linda Yin, MD**, **Madhavi Duvvuri, MPhil, BA**, **Michael Feeley, BS**, and **Alexander T. Hillel, MD, FACS**

Johns Hopkins School of Medicine, Department of Otolaryngology (M.K.M., K.M.M., D.D., L.Y., M.D., M.F., A.T.H.), Baltimore, Maryland, U.S.A

Abstract

Objective—Management of laryngotracheal stenosis (LTS) remains primarily surgical, with a critical need to identify targets for adjuvant therapy. Laryngotracheal stenosis scar fibroblasts exhibit a profibrotic phenotype with distinct metabolic shifts, including an increased glycolysis/oxidative phosphorylation ratio. This study examines the effects of the glutamine antagonist 6-diazo-5-oxo-l-norleucine (DON) on collagen production, gene expression, proliferation, and metabolism of human LTS-derived fibroblasts in vitro.

Method—Paired normal and scar-derived fibroblasts isolated from subglottic and proximal tracheal tissue in patients with iatrogenic laryngotracheal stenosis (iLTS) were cultured. Proliferation rate, gene expression, protein production, and cellular metabolism were assessed in two conditions: 1) fibroblast growth medium, and 2) fibroblast growth medium with 1×10^{-4} M DON.

Results—DON treatment reduced cellular proliferation rate ($n = 7$, $P = 0.0150$). Expression of genes collagen 1 and collagen 3 both were reduced ($n = 7$, $P = 0.0102$, 0.0143, respectively). Soluble collagen production decreased ($n = 7$, $P = 0.0056$). As measured by the rate of extracellular acidification, glycolysis and glycolytic capacity decreased ($n = 7$, $P = 0.0082$, 0.0003, respectively). adenosine triphosphate (ATP) production and basal respiration decreased ($n = 7$, $P = 0.0045$, 0.0258, respectively), determined by measuring the cellular rate of oxygen consumption.

Conclusion—The glutamine antagonist DON reverses profibrotic changes by inhibiting both glycolysis and oxidative phosphorylation in iLTS scar fibroblasts. In contrast to untreated iLTS scar fibroblasts, collagen gene expression, protein production, metabolic rate, and proliferation were significantly reduced. These results suggest DON and/or its derivatives as strong candidates for adjuvant therapy in the management of iatrogenic laryngotracheal stenosis. Enzymes involved in glutamine metabolism inhibited by DON offer targets for future investigation.

Level of Evidence—NA.

Send correspondence to Alexander Hillel, 601 N. Caroline St, 6th Floor, Baltimore, MD 21287. ahillel@jhmi.edu.

Additional supporting information may be found in the online version of this article.

Presented at the American Broncho–Esophagological Association (ABEA) in conjunction with the Combined Otolaryngology Spring Meetings (COSM), San Diego, California, U.S.A., April 26–30, 2017.

The authors have no other funding, financial relationships, or conflicts of interest to disclose.

Keywords

Human; trachea; stenosis; iatrogenic; larynx; laryngotracheal stenosis; fibroblasts; collagen; scar; fibrosis; glutamine; glutamine antagonism; aerobic glycolysis; metabolism; metabolic inhibitor

Introduction

Laryngotracheal stenosis (LTS) is a morbid, potentially life-threatening fibrotic condition that leads to progressive narrowing of the glottic and/or tracheal airway.[1–4] Diverse etiologies give rise to LTS, including congenital, autoimmune, idiopathic, and iatrogenic LTS. Congenital tracheal stenosis (CTS) remains ill-defined while encompassing a range of pathologies. Predominantly due to complete tracheal rings, CTS may involve anywhere from a short segment to the entire trachea, and frequently is associated with other congenital anatomical defects (70% to 90% of CTS cases).[5] In contrast to CTS, autoimmune and idiopathic LTS affect the mucosa, and iatrogenic may involve both.[6,7] The most predominant etiology of LTS is iatrogenic (iLTS), in which intubation injury to the epithelium promotes prolonged subepithelial inflammation and subsequently fibroblast proliferation and collagen deposition.[1,3,8] This dysregulated wound-healing response is driven by complex signaling between epithelial cells, immune mediators, and fibroblasts, which stimulates deposition of excessive collagen, leading to airway narrowing.[9–11] Mild airway restriction secondary to this narrowing impacts quality of life, and in severe cases requires surgical intervention to relieve the resultant dyspnea. Although adjuvant medical therapies such as steroids exist, cricotracheal or tracheal resection—with their associated morbidity and mortality—are the only definitive treatments for this disease.[12] Given the risks of surgery and ineffective medical options, there is a definite need for investigation into an effective medical therapy for iLTS.

To transition from surgical to medical management, novel therapies must be developed. Addressing this clinical need reveals a knowledge gap in our understanding of the pathophysiology of iLTS. Because iLTS is a disease hallmarked by excessive collagen deposition, fibroblasts are thought to be the primary effector cell. However, the underlying differences in these fibroblasts are poorly understood, including biologic and metabolic differences between scar and normal laryngotracheal fibroblasts. Recent evidence indicates that there are distinct abnormalities in iLTS scar fibroblasts when compared to normal airway fibroblasts from the same patient.[13] iLTS scar fibroblasts are hyperproliferative, have increased extracellular matrix (ECM) deposition, and demonstrate a metabolic shift to reduced oxidative phosphorylation and increased aerobic glycosis.[13–15] A similar phenotype wherein hyperproliferation is driven by aerobic glycolysis is seen in fibrosis of other organs, as in the case of idiopathic pulmonary fibrosis (IPF).[14,16,17] In IPF, fibroblasts demonstrate changes that favor uncontrolled proliferation and ECM synthesis,[18] supported by glycolytic reprogramming.[14] Moreover, previous investigation has shown that targeting cellular metabolism with rapamycin reduces proliferation, collagen 1 (COL1) gene expression, and collagen deposition in iLTS scar fibroblasts.[19] Rapamycin inhibits the mechanistic target of rapamycin, a ubiquitous protein with many cellular functions, including regulation of cellular metabolism, nucleotide biosynthesis, immune cell activation, and cell growth and

proliferation.[20,21] Additionally, bioenergetic analysis of iLTS scar fibroblasts treated with rapamycin revealed reduced oxidative phosphorylation, demonstrating a relationship between cellular metabolism and fibrosis, potentially revealing metabolic inhibition as a therapeutic target in iLTS.[19]

Metabolic inhibition has shown promise as an adjuvant therapy for cancer and IPF, conditions both defined by cellular hyperproliferation.[14,15] Proliferation requires increased uptake of glutamine, which becomes an essential amino acid under these conditions.[17] Enzymes responsible for processing glutamine can be inhibited by 6-diazo-5-oxo-l-norleucine (DON), a metabolic inhibitor synthesized by *Streptomyces ambofaciens*.[22,23] DON-mediated glutamine antagonism has demonstrated therapeutic potential in diverse conditions driven by hyperproliferative cells, including glioblastoma; cerebral malaria; viral encephalomyelitis; and recently, pulmonary fibrosis.[15,24–26] In each, the DON-induced glutamine shortage inhibits proliferation of either pathologic neoplastic cells or immune mediators. Glutamine deprivation is tolerated by normal tissue but can be lethal to rapidly proliferating, dysregulated cells.[27–29] Hyperproliferative fibroblasts demonstrate aerobic glycolysis and increased glutamine uptake,[17] which may leave them vulnerable to inhibition of glutamine metabolism. Given these recent findings and our understanding of iLTS scar fibroblast metabolism, we hypothesize that glutamine inhibition will reduce or reverse fibrosis in iLTS fibroblasts in vitro. In turn, we test the null hypothesis that glutamine inhibition does not affect fibrotic behavior of iLTS fibroblasts. To investigate this hypothesis, a series of controlled in vitro experiments were performed on paired human fibroblasts derived from normal and iLTS scar tissue. Scar fibroblasts were treated with DON, and treatment efficacy was determined by assessing proliferation, morphology, gene expression, collagen production, and cellular metabolic profile compared with untreated scar fibroblasts, as well as normal fibroblasts from the same patient.

Materials and Methods

Patient Recruitment

Participants in this study were consecutive patients diagnosed with iLTS and treated by a single surgeon. All were willing participants who completed an institutional review board-approved informed consent process. Inclusion criteria were: 18 years of age or greater and diagnosis of acquired iLTS. Exclusion criteria were age less than 18 years and active pregnancy. Patient demographics, disease characteristics, comorbidities, and relevant history were evaluated to determine homogeneity of cohort.

Laryngotracheal Fibroblast Isolation and Culture

Biopsies of fibrotic subglottic or cervical tracheal tissue, as well as normal healthy tissue from the distal trachea, were harvested from the same patient during scheduled suspension microlaryngoscopy. Informed consent was obtained from participants, as approved by the Johns Hopkins Institutional Review Board (NA_00078310). All biopsies were obtained by the same surgeon, with source tissue initially identified by visual inspection. Primary fibroblasts were isolated from the biopsy specimens, cultured, and expanded—and then

experiments were performed with passage 2 or 3 cells, as in earlier work.[13,19] Cellular phenotype was confirmed through immunohistochemical staining, as previously described.[19]

Experimental Conditions

Cells were grown in vitro in three conditions: Condition 1 consisted of normal, nonscar fibroblasts in normal fibroblast growth media, as previously described.[19] iLTS scar fibroblasts were grown in normal media (condition 2) and media with 1×10^{-4} M DON (condition 3). DON was acquired from Sigma Aldrich (catalog number D2141; Sigma Aldrich, St. Louis, Missouri, U.S.A.).

Cell Proliferation by MTS Assay

Normal and iLTS scar fibroblasts were grown to confluence, trypsinized, and plated in 96-well culture plates (Falcon; BD Biosciences, San Jose, California, U.S.A.) with fibroblast growth medium at 1×10^4 cells per well in conditions 1, 2, and 3, as described in experimental conditions above. After 72 hours incubation, cells were treated with MTS Colorimetric Assay (Abcam, Cambridge, U.K.) per manufacturer protocol. Absorbance was measured with a BioTek Synergy 2 Microplate Reader (BioTek Instruments, Winooski, Vermont, U.S.A.) at optical density (OD) of 490 nm. Each sample was run in triplicate.

Morphology by Masson's Trichrome Stain

iLTS scar fibroblasts were plated at 3×10^4 cells per well and cultured in conditions 2 and 3 on gelatin-coated microscope slide cover slips for 72 hours. Masson's Trichrome Stain (Sigma Aldrich, catalog number HT15-1KT) was applied, as previously described.[19] Photomicrographs of representative sections were obtained with a Zeiss Axioimager A2 (Carl Zeiss AG, Oberkochen, Germany).

Gene Expression Analysis by Real-Time Polymerase Chain Reaction

Paired normal and iLTS scar fibroblasts were seeded in six-well culture plates (Falcon, BD Biosciences) at 2×10^5 cells per well in triplicate and incubated for 72 hours in conditions 1, 2, and 3. RNA extraction, cDNA synthesis, and qualitative real-time polymerase chain reaction were completed, as previously described[30]. Condition 1 cells from the same patient were used as controls. β actin (ACTB) was used as the housekeeping gene for all samples. Expression of the target gene was calculated using the $2^{-\Delta\Delta C\tau}$ method. Error was calculated as the standard error of the mean (SEM) of $\Delta\Delta C\tau$. Genes of interest were COL1, collagen 3 (COL3), fibronectin 1 (FN1), matrix metallopeptidase 13 (MMP13), and transforming growth factor β (TGFB1). Primers for all gene targets were supplied by Integrated DNA Technologies (IDT, Coralville, Indiana, U.S.A.).

Soluble Collagen Production Analysis

Paired normal and iLTS scar fibroblasts were cultured, as described in Gene Expression. Following 72 hours of incubation, one milliliter (mL) of media from each well was transferred to a low-protein binding 1.5 mL microcentrifuge tube (Lo-Bind; Eppendorf, Hamburg, Germany) and processed using the Sircol Soluble Collagen Assay (Biocolor,

Carrickfergus, U.K.). Sample absorbance was measured using a BioTek Synergy 2 Microplate Reader (BioTek) at OD of 555 nm.

Cellular Metabolism Using Oxygen Consumption Rate Measurements

Individual cell metabolism may be characterized by observing the oxygen consumption rate (OCR) of cells in response to inhibitors of oxidative phosphorylation[33]. The Seahorse XF24 Flux Analyzer (Agilent Technologies, Santa Clara, California, U.S.A.) permits whole-cell mitochondrial analysis. Scar fibroblasts were seeded in 24-well Seahorse culture plates (Agilent Technologies) in conditions 2 and 2 at 3×10^4 cells per well. All conditions were run six times. Cells were incubated in experimental conditions for 72 hours, with media exchange every 24 hours. At the end of this incubation, the OCR was analyzed with a Seahorse XF24 Flux Analyzer (Agilent Technologies), as previously described[13].

Cellular Glycolysis Using Extracellular Acidification Rate

Glycolysis leads to extrusion of protons into the extracellular environment, altering the pH. The Seahorse XF24 Flux Analyzer (Agilent Technologies) measures the extracellular acidification rate as inhibitors of glycolysis are sequentially added to the growth environment of whole cells, determining their glycolytic properties. iLTS scar fibroblasts were plated, treated, and incubated, as described in cellular metabolism using oxygen consumption rate measurements. Analysis proceeded as in prior research[13].

Statistical Analysis

All results were collected and organized using Microsoft Excel (Microsoft 2016, Redmond, Washington, U.S.A.). Statistical tests were completed using Prism 6.06 (Graphpad, La Jolla, California, U.S.A.). Results were expressed as mean, mean difference, range, 95% confidence interval (CI), and SEM. Statistical analysis was performed using paired Student *t* test. Results were considered statistically significant at $P \leq 0.05$ (*), $P \leq 0.01$ (**), and $P \leq 0.001$ (***). A Bonferroni correction was implemented when the three conditions were analyzed for two comparisons ($P \leq 0.025$ [*], $P \leq 0.005$ [**], and $P \leq 0.0005$ [***]) or for three comparisons ($P \leq 0.0166$ [*], $P \leq 0.0033$ [**], and $P \leq 0.0003$ [***]).

Results

Experimental Cohort

Biopsies were taken from seven individuals who were enrolled in this study. Fibroblasts from normal and scar tracheal epithelia were studied in pairs, by source patient. Results were averaged by category across patients. Evaluation of demographics, disease characteristics, comorbidities, and patient history revealed good homogeneity with regard to disease. Findings are summarized in Table I.

DON Reduces iLTS Scar Fibroblast Hyperpro-liferation—Relative to normal fibroblasts, iLTS scar fibroblasts proliferate at a significantly higher rate, with a mean percentage difference of 26.14%, 95% CI of 8.63% to 43.65%, SEM of ± 7.16, $n = 7$, and $P = 0.010$. Treatment of iLTS fibroblasts with DON reduced the rate of proliferation (mean percentage difference −16.43%, 95% CI: −2.932% to −29.92%, SEM ± 5.52, $n = 7$, $P =$

0.0244). Representative images of treated and untreated iLTS scar fibroblasts obtained using Masson's Trichrome Stain (Sigma Aldrich) demonstrate alteration in proliferation and morphology. Proliferation rate and histology results are summarized in Figure 1. All results were normalized to proliferation rates of normal fibroblasts from the same patient. Untreated scar fibroblasts proliferated at a mean of 126% (range 104% to 158%, 95% CI: 113% to 139%, SEM ± 7%) relative to the rate of normal fibroblasts. Treatment with DON reduced the proliferation rate to a mean of 110% (range 68% to 159%, 95% CI: 90% to 129%, SEM ± 10%). Patient-specific results are presented in Figure 1D. The proliferation rate of iLTS scar fibroblasts treated with DON was not significantly different from normal fibroblasts.

DON-Treated iLTS Scar Fibroblasts Demonstrate Reduced COL1, COL3 Expression—Normal, nonscar airway fibroblasts were used as controls for analysis. Real-time polymerase chain reaction analysis revealed that DON treatment of iLTS scar fibroblasts decreased the expression of genes COL1 (mean fold change for untreated scar fibroblasts: 2.25, range 0.49 to 4.35, 95% CI: 1.41 to 3.08, SEM ± 0.43; mean fold change for DON-treated scar fibroblasts: 1.18, range 0.41 to 1.73, 95% CI: 0.89 to 1.47, SEM ± 0.15) and COL3 (mean fold change for untreated scar fibroblasts: 1.31, range 0.54 to 2.24, 95% CI: 0.92 to 1.7, SEM ± 0.20; mean fold change for DON-treated scar fibroblasts 0.94, range 0.32 to 3.03, 95% CI 0.30 to 1.58, SEM ± 0.33) in scar tissue (mean fold change difference −0.5724, 95% CI: −0.3953 to −0.8286, $n = 7$, $P = 0.0102$; and −0.6068, 95% CI: −0.4240 to −0.8685, $n = 7$, $P = 0.0143$, respectively). iLTS scar fibroblast expression of COL1 and COL3 was not different from normal fibroblasts after treatment with DON. Expression of FN1, MMP13, and TGF β did not change in iLTS-scar fibroblasts following treatment with DON. Results are summarized in Figure 2. Patient-specific results are displayed in the Supporting Figure S1.

DON Reduces Elevated Production of Soluble Collagen by iLTS Scar Fibroblasts—There was an increase in soluble collagen produced by iLTS scar fibroblasts when compared to normal fibroblasts. Collagen production was measured in μg/mL. Mean collagen production for normal fibroblasts was 14.23 μg/mL, range 6.68 to 30.33 μg/mL, 95% CI: 8.52 to 19.92 μg/mL, SEM ± 2.91. Mean untreated scar fibroblast collagen production was 18.61 μg/mL, range 8.75 to 38.45 μg/mL, 95% CI: 11.96 to 25.26, SEM ± 3.39. DON-treated iLTS scar fibroblasts produced a mean of 11.86 μg/mL, range 4.60 to 20.09 μg/mL, 95% CI: 8.07 to 15.67 μg/mL, SEM ± 1.93. Comparing normal and iLTS scar fibroblasts reveals a mean difference of 4.38 μg/mL, with 95% CI: 2.81 to 5.95, SEM of ± 0.80 μg/mL, $n = 7$, and $P = 0.002$. The mean difference between untreated and treated iLTS scar fibroblast collagen production was −6.74 μg/mL, 95% CI −10.46 to −3.02 μg/mL, SEM ± 5.02 μg/mL, n57, P50.0167. DON-treated iLTS scar fibroblasts produced soluble collagen at levels similar to normal fibroblasts. Figure 3 displays individual subject results and summarizes the findings, showing that treatment with DON reduces soluble collagen production by iLTS scar fibroblasts.

DON Alters the Metabolic Behavior of iLTS Scar Fibroblasts—Comparison of the metabolic profile of iLTS scar fibroblasts with and without DON treatment found reductions in glycolysis (mean glycolysis rate of untreated scar fibroblasts 10.04, range 3.40 to 20.40,

95% CI: 5.15 to 14.93, SEM ± 2.50; mean rate for DON-treated scar fibroblasts 7.50, range 1.58 to 18.13, 95% CI: 2.91 to 12.07, SEM ± 2.34; mean difference −2.546, 95% CI: −4.151 to −0.941, $n = 7$, $P = 0.0082$), and glycolytic capacity (mean glycolytic capacity of untreated scar fibroblasts 9.65, range 5.21 to 15.39, 95% CI: 6.90 to 12.40, SEM ± 1.40; mean capacity for DON-treated scar fibroblasts 5.99, range 1.76 to 11.89, 95% CI: 3.51 to 8.46, SEM ± 1.26; mean difference −3.665, 95% CI: −4.842 to −2.489, $n = 7$, $P = 0.0003$) following treatment with DON (Fig. 4). Mitochondrial respiration analysis found DON treatment-reduced iLTS scar fibroblast ATP production (mean ATP production of untreated scar fibroblasts 41.81, range 18.55 to 69.13, 95% CI: 28.80 to 54.82, SEM ± 6.64; mean production for DON-treated scar fibroblasts 25.10, range 5.31 to 54.72, 95% CI: 13.53 to 36.67, SEM ± 5.90; mean difference −16.71, 95% CI: −25.97 to −7.44, $n = 7$, $P = 0.0045$) and basal respiration (mean basal respiration of untreated scar fibroblasts 62.08, range 39.23 to 91.22, 95% CI: 47.65 to 76.52, SEM ± 7.37; mean basal respiration for DON-treated scar fibroblasts 43.85, range 23.87 to 66.61, 95% CI: 32.28 to 55.41, SEM ± 5.90; mean difference −18.23, 95% CI: −33.79 to −2.676, $n = 7$, $P = 0.0285$), shown in Figure 5.

Discussion

In this study, iLTS scar fibroblasts exhibit a hyperfunctional phenotype characterized by rapid proliferation and altered gene expression, leading to increased collagen deposition compared with normal fibroblasts from the same patient. These functional changes in iLTS scar fibroblasts were previously shown to be associated with increased aerobic glycolysis.[13] In the current study, glutamine antagonism by DON reduced iLTS scar fibroblast proliferation, COL1 and COL3 gene expression, and soluble collagen production. Moreover, glycolysis and oxidative phosphorylation decreased following treatment with DON. These findings indicate that the profibrotic phenotype associated with iLTS scar fibroblasts may be reversed through metabolic reprogramming with glutamine antagonism.

The metabolic profile of scar fibroblasts observed in this study is consistent with previous investigations of iLTS and IPF fibroblasts, which demonstrated that increased utilization of aerobic glycolysis exists in hyperproliferative profibrotic fibroblasts.[13–15] Rapid protein synthesis and cell division, such as seen in this study, require significant de novo macromolecular building blocks, which are supported by aerobic glycolysis wherein glycolytic products are redirected to biosynthesis rather than the tricarboxylic acid (TCA) cycle. To maintain levels of TCA cycle intermediates, cells rely on glutamine anaplerosis, making glutamine an essential amino acid under these conditions.[17] This glutamine-derived support of the TCA cycle is inhibited by DON, limiting cellular options for anaplerosis. Shortage of TCA cycle intermediates may limit both energy production and biosynthetic reactions, which extensively utilize these compounds. Given the critical roles that energy production and biosynthesis play in iLTS-scar fibroblast proliferation and collagen production, their reduction with DON treatment suggest that glutamine metabolism is integral to the fibrotic phenotype and that its inhibition may be a potential therapy for iatrogenic LTS.

Depriving pathologic cells of glutamine is not a new concept. Although DON has contributed to recent scientific advances, it was first isolated in the 1950s and tested as a

chemotherapeutic. It reduced tumor burden but was abandoned due to intolerable side effects.[34] Despite this, glutamine inhibition remains a promising mechanism, with new investigations focusing on maintaining DON efficacy while ameliorating side effects.[24,35] This recently has been accomplished with the development of DON prodrugs.[24] Although this study supports the potential of these prodrugs, further elucidation of glutamine's role in fibrosis and the effects of antagonism is required, which may be accomplished by studying the metabolomics of iLTS scar fibroblasts.

Metabolomics is the study of metabolites involved in cellular processes and offers the ability to characterize changes to individual metabolic pathways. Although we demonstrate that inhibition of glutamine metabolism reverses the profibrotic phenotype of iLTS fibroblasts, DON inactivates a diverse set of glutamine-processing enzymes. It remains to be determined which enzymes are essential to fibrosis and which pathways are unnecessarily blocked. It may be that targeting a subset of DON-effected enzymes would yield therapeutic benefit while minimizing adverse effects. Selecting candidate enzymes for inhibition requires a better understanding of differences in enzyme expression and activity between normal, iLTS scar, and glutamine-deprived iLTS scar fibroblasts. Tracking glutamine flux through the cell by examining related protein expression and the relative levels of metabolites will reveal the shifts in metabolic machinery associated with the fibrotic phenotype. Those specific proteins identified through this process may yield therapeutic targets for iLTS and fibrosis in general.

Although these results are encouraging and contribute to our understanding of laryngotracheal stenosis, this study has limitations. Despite the fact that in vitro findings do not correlate perfectly with in vivo physiology, this work offers insights on the effect of glutamine antagonism on pathologic fibroblasts, which can be leveraged for further in vitro and in vivo work. One cause of variation between in vitro and in vivo observations is cellular dedifferentiation in response to in vitro culture methods such as freeze–thaw cycles and passaging. To limit these effects, experiments used only cells that had been passaged two or three times. Because significant variation exists between patients, paired normal and pathologic tissue was acquired from each patient, and experiments were completed on paired samples. When all patients were averaged, significant differences were seen in the outcome measures.

Conclusion

Glutamine inhibition reverses the fibrotic behavior of iLTS scar fibroblasts in vitro, rejecting the null hypothesis. We demonstrate that blocking glutamine metabolism with DON reverses the profibrotic phenotype of iLTS scar fibroblasts in vitro, with reductions in proliferation, gene expression, ECM deposition, and metabolic activity. Further investigation into dysregulated glutamine metabolism in iLTS scar fibroblasts may yield specific targets within glutamine metabolism pathways that could translate into effective medical therapy for iLTS.

Acknowledgments

Research reported in this publication was supported by National Institute on Deafness and Other Communication Disorders of the National Institutes of Health (NIH) under award number 1K23DC014082 (A.T.H.). The content is solely the responsibility of the authors and does not necessarily represent the official views of the NIH. This study

also was financially supported by the Triological Society and American College of Surgeons (A.T.H.), as well as by a T32 NIH training grant (K.M.M.).

Bibliography

1. Ghosh A, Malaisrie N, Leahy KP, et al. Cellular adaptive inflammation mediates airway granulation in a murine model of subglottic stenosis. Otolaryngol Head Neck Surg. 2011; 144:927–933. [PubMed: 21493347]
2. Hillel AT, Namba D, Ding D, Pandian V, Elisseeff JH, Horton MR. An in situ, in vivo, murine model for the study of laryngotracheal stenosis. JAMA Otolaryngol Head Neck Surg. 2014; 140:961–966. [PubMed: 25144860]
3. Minnigerode B, Richter HG. Pathophysiology of subglottic tracheal stenosis in childhood. Prog Pediatr Surg. 1987; 21:1–7.
4. Rockey DC, Bell PD, Hill JA. Fibrosis—a common pathway to organ injury and failure. N Engl J Med. 2015; 372:1138–1149. [PubMed: 25785971]
5. Hofferberth SC, Watters K, Rahbar R, Fynn-Thompson F. Management of congenital tracheal stenosis. Pediatrics. 2015; 136:e660–e669. [PubMed: 26304826]
6. Costantino CL, Mathisen DJ. Idiopathic laryngotracheal stenosis. J Thorac Dis. 2015; 8(suppl 2):S204–S209.
7. Gelbard A, Francis DO, Sandulache VC, Simmons JC, Donovan DT, Ongkasuwan J. Causes and consequences of adult laryngotracheal stenosis. Laryngoscope. 2015; 125:1137–1143. [PubMed: 25290987]
8. Gadkaree SK, Pandian V, Best S, et al. Laryngotracheal stenosis. Otolaryngol Head Neck Surg. 2017; 156:321–328. [PubMed: 28112014]
9. Sakai N, Tager AM. Fibrosis of two: epithelial cell-fibroblast interactions in pulmonary fibrosis. Biochim Biophys Acta. 2013; 1832:911–921. [PubMed: 23499992]
10. Gelbard A, Katsantonis NG, Mizuta M, et al. Molecular analysis of idiopathic subglottic stenosis for Mycobacterium species. Laryngoscope. 2017; 127:179–185. [PubMed: 27295947]
11. Gelbard A, Katsantonis NG, Mizuta M, et al. Idiopathic subglottic stenosis is associated with activation of the inflammatory IL-17A/IL-23 axis. Laryngoscope. 2016; 126:E356–E361. [PubMed: 27296163]
12. Herrington HC, Weber SM, Andersen PE. Modern management of laryngotracheal stenosis. Laryngoscope. 2006; 116:1553–1557. [PubMed: 16954977]
13. Ma G, Samad I, Motz K, et al. Metabolic variations in normal and fibrotichuman laryngotracheal-derived fibroblasts: a Warburg-like effect. Laryngoscope. 2017; 127:E107–E113. [PubMed: 27585358]
14. Xie N, Tan Z, Banerjee S, et al. Glycolytic Reprogramming in myofibroblast differentiation and lung fibrosis. Am J Respir Crit Care Med. 2015; 192:1462–1474. [PubMed: 26284610]
15. Viegland CL, Chan-Li Y, Collins SL, et al. Inhibition of glutamine metabolism arrests the development of pulmonary fibrosis. In ATS Conference 2016, C37 Pulmonary Fibrosis. Am J Respir Crit Care Med. 2016; 193:A4935.
16. Vander Heiden MG, Cantley LC, Thompson CB. Understanding the Warburg effect: the metabolic requirements of cell proliferation. Science. 2009; 324:1029–1033. [PubMed: 19460998]
17. Ghesquiere B, Wong BW, Kuchnio A, Carmeliet P. Metabolism of stromal and immune cells in health and disease. Nature. 2014; 511:167–176. [PubMed: 25008522]
18. Ramos C, Montano M, Garcia-Alvarez J, et al. Fibroblasts from idiopathic pulmonary fibrosis and normal lungs differ in growth rate, apoptosis, and tissue inhibitor of metalloproteinases expression. Am J Respir Cell Mol Biol. 2001; 24:591–598. [PubMed: 11350829]
19. Namba DR, Ma G, Samad I, et al. Rapamycin inhibits human laryngotracheal stenosis-derived fibroblast proliferation, metabolism, and function in vitro. Otolaryngol Head Neck Surg. 2015; 152:881–888. [PubMed: 25754184]
20. Hay N, Sonenberg N. Upstream and downstream of mTOR. Genes Dev. 2004; 18:1926–1945. [PubMed: 15314020]

21. Jaeschke, A., Dennis, PB., Thomas, G. mTOR: A mediator of intracellular homeostasis. In: Thomas, G.Sabatini, DM., Hall, MN., editors. TOR: Target of Rapamycin. Berlin, Heidelberg, Germany: Springer; 2004. p. 283-298.
22. Pettit GR, Nelson PS. Synthesis of the streptomyces ambofaciens antineo-plastic constituent 6-diazo-5-oxo-L-norleucine. J Org Chem. 1983; 48:741–744.
23. Pinkus LM. Glutamine binding sites. Methods Enzymol. 1977; 46:414–427. [PubMed: 909432]
24. Rais R, Jancarik A, Tenora L, et al. Discovery of 6-Diazo-5-oxo-l-norleucine (DON) prodrugs with enhanced CSF delivery in monkeys: a potential treatment for glioblastoma. J Med Chem. 2016; 59:8621–8633. [PubMed: 27560860]
25. Manivannan S, Baxter VK, Schultz KLW, Slusher BS, Griffin DE. Protective effects of glutamine antagonist 6-diazo-5-oxo-l-norleucine in mice with alphavirus encephalomyelitis. J Virol. 2016; 90:9251–9262. [PubMed: 27489275]
26. Gordon EB, Hart GT, Tran TM, et al. Targeting glutamine metabolism rescues mice from late-stage cerebral malaria. Proc Natl Acad Sci U S A. 2015; 112:13075–13080. [PubMed: 26438846]
27. Hensley CT, Wasti AT, DeBerardinis RJ. Glutamine and cancer: cell biology, physiology, and clinical opportunities. J Clin Invest. 2013; 123:3678–3684. [PubMed: 23999442]
28. Yuneva M, Zamboni N, Oefner P, Sachidanandam R, Lazebnik Y. Deficiency in glutamine but not glucose induces MYC-dependent apoptosis in human cells. J Cell Biol. 2007; 178:93–105. [PubMed: 17606868]
29. Lacey JM, Wilmore DW. Is glutamine a conditionally essential amino acid? Nutr Rev. 1990; 48:297–309. [PubMed: 2080048]
30. Hillel AT, Varghese S, Petsche J, Shamblott MJ, Elisseeff JH. Embryonic germ cells are capable of adipogenic differentiation in vitro and in vivo. Tissue Eng Part A. 2009; 15:479–486. [PubMed: 18673089]
31. Livak KJ, Schmittgen TD. Analysis of relative gene expression data using real-time quantitative PCR and the 2(-Delta Delta C(T)) method. Methods. 2001; 25:402–408. [PubMed: 11846609]
32. Hillel AT, Unterman S, Nahas Z, et al. Photoactivated composite biomaterial for soft tissue restoration in rodents and in humans. Sci Transl Med. 2011; 3:93ra67.
33. Schuh RA, Clerc P, Hwang H, et al. Adaptation of microplate-based respirometry for hippocampal slices and analysis of respiratory capacity. J Neurosci Res. 2011; 89:1979–1988. [PubMed: 21520220]
34. Magill GB, Myers WPL, Reilly HC, et al. Pharmacological and initial therapeutic observations on 6-Diazo-5-Oxo-L-Norleucine (Don) in human neoplastic disease. Cancer. 1957; 10:1138–1150. [PubMed: 13489662]
35. Ovejera AA, Houchens DP, Catane R, Sheridan MA, Muggia FM. Efficacyof 6-Diazo-5-oxo-l-norleucine and N-[N-γ-Glutamyl-6-diazo-5-oxo-norleu-cinyl]-6-diazo-5-oxo-norleucine against experimental tumors in conventional and nude mice. Cancer Res. 1979; 39:3220–3224. [PubMed: 572261]

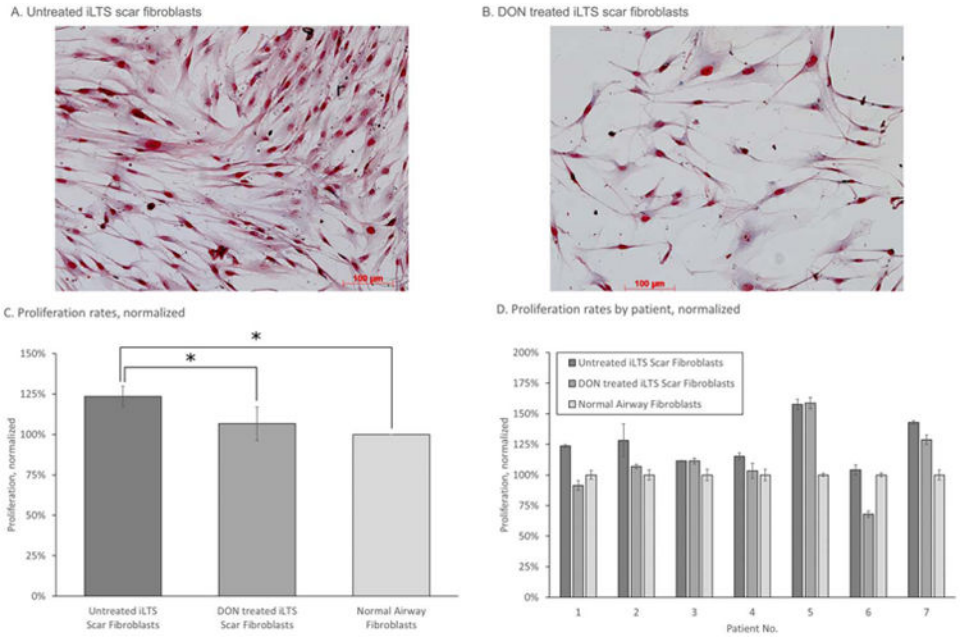

Fig. 1.

DON inhibits the hyperproliferative behavior of iLTS scar fibroblasts seen in (A). Representative Masson's Trichrome Stain (Sigma Aldrich, St. Louis, Missouri, U.S.A.) of untreated iLTS scar fibroblasts, which contrasts with (B). Masson's trichrome stain of iLTS scar fibroblasts treated with DON. (C) Results of DON treatment on proliferation rate of iLTS scar fibroblasts, compared to untreated iLTS scar fibroblasts. DON-treated iLTS scar fibroblast proliferation rate does not significantly differ from the proliferation rate of normal fibroblasts. DON = 6-diazo-5-oxo-l-norleucine; iLTS = iatrogenic laryngotracheal stenosis. [Color figure can be viewed in the online issue, which is available at www.laryngoscope.com.]

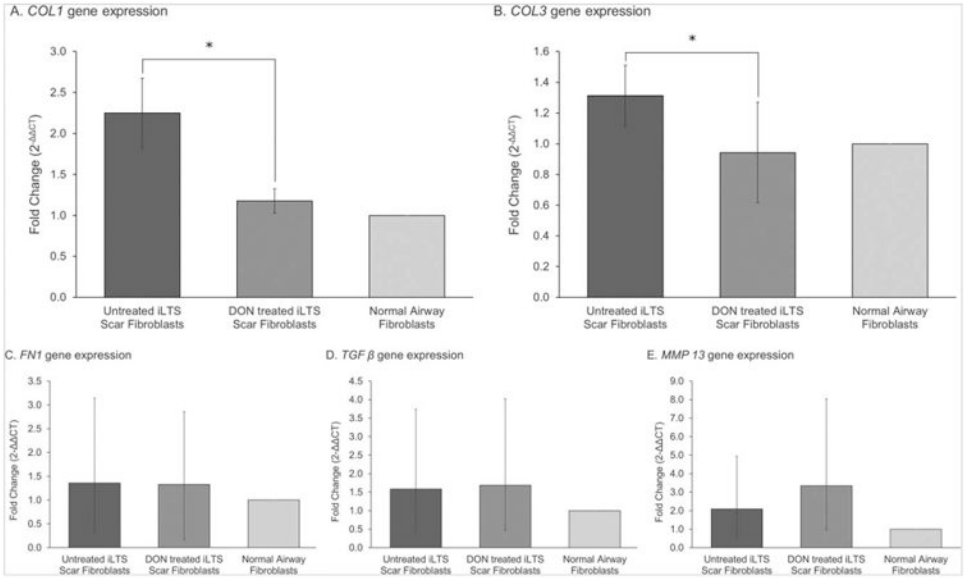

Fig. 2.

DON treatment of iLTS scar fibroblasts reduces collagen gene expression. DON treatment significantly reduces the expression of COL1 and COL3 in iLTS scar fibroblasts, compared to untreated iLTS scar fibroblasts. DON-treated iLTS scar fibroblast expression of COL1 and COL3 are not significantly different from normal fibroblast expression levels.

COL1 = collagen 1; COL3 = collage 3; DON = 6-diazo-5-oxo-l-norleucine; FN1 = fibronectin 1; iLTS = iatrogenic laryngotracheal stenosis; MMP 13 = matrix metallopeptidase 13; TGF β = transforming growth factor beta.

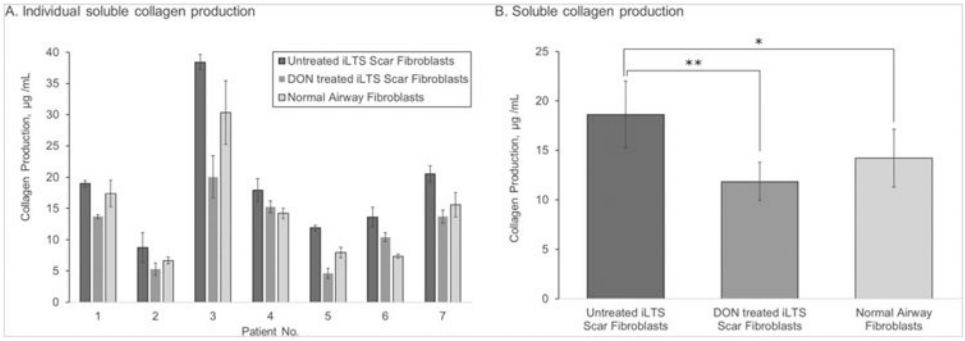

Fig. 3.

DON reduces soluble collagen production in iLTS fibroblasts. In (A), soluble collagen production is reported on a per-subject basis. Soluble collagen production by iLTS scar fibroblasts is significantly greater than normal fibroblasts. Treatment with DON significantly reduces collagen production of iLTS scar fibroblasts. Rates of soluble collagen production by DON-treated iLTS scar fibroblasts and normal fibroblasts are not significantly different. (B) An averaged view of the individual results.

DON = 6-diazo-5-oxo-l-norleucine; iLTS = iatrogenic laryngotracheal stenosis.

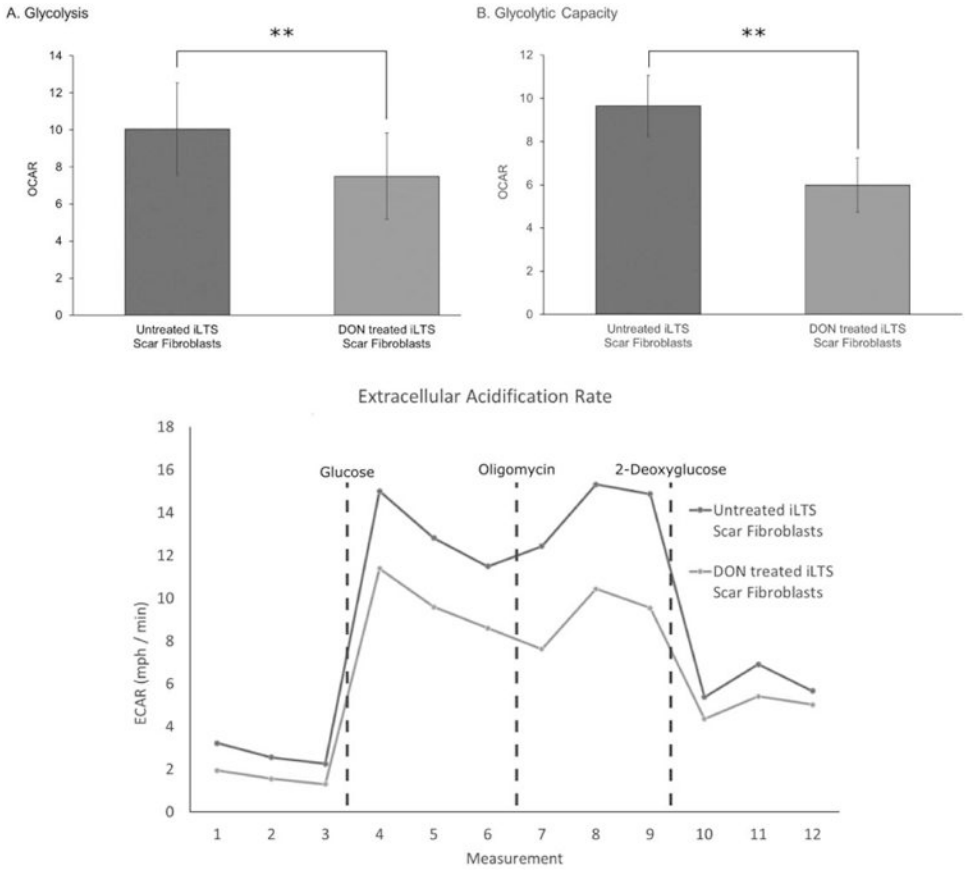

Fig. 4.

DON reduces glycolysis and glycolytic capacity in iLTS fibroblasts. (A) Comparison of the glycolysis rates of untreated iLTS scar fibroblasts to those of DON-treated iLTS fibroblasts, demonstrating significantly lower glycolysis than untreated iLTS scar fibroblasts as measured by the change in ECAR. (B) A similar result is revealed for glycolytic capacity, wherein DON-treated iLTS scar fibroblasts have significantly less glycolytic capacity than untreated iLTS scar fibroblasts. (C) The ECAR of untreated and DON-treated iLTS scar fibroblasts during the Seahorse XF24 (Agilent Technologies, Santa Clara, California, U.S.A.) experiment are displayed.

DON = 6-diazo-5-oxo-l-norleucine; ECAR = extracellular acidification rate; iLTS = iatrogenic laryngotracheal stenosis.

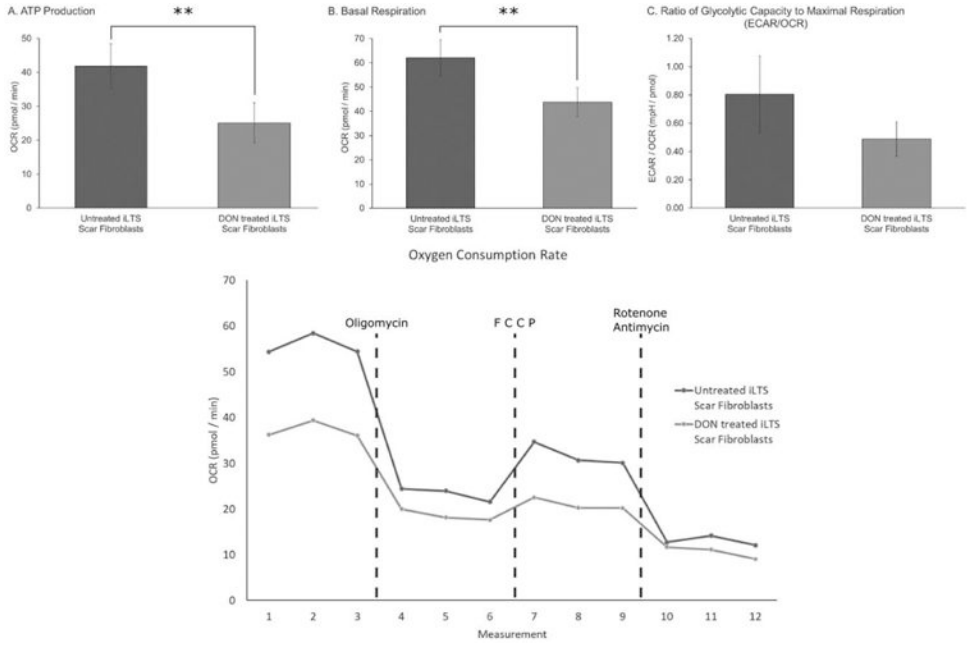

Fig. 5.

DON reduces ATP production and basal respiration, measurements of oxygen consumption rate. (A) The ATP production of untreated iLTS scar fibroblasts contrasts with that of DON-treated iLTS scar fibroblasts, revealing a significant reduction with DON exposure as measured by changes in the OCR. (B) Displays the effects on basal respiration, which is significantly reduced in DON-treated iLTS scar fibroblasts compared to untreated iLTS scar fibroblasts. (C) The ratio of the ECAR to OCR shows a trend toward reduction in iLTS scar fibroblasts following treatment with DON, which did not reach significance within this limited cohort. (D) As in (C), (D) depicts the OCR measures for iLTS scar fibroblasts with and without DON treatment during a Seahorse XF24 (Agilent Technologies, Santa Clara, California, U.S.A.) experiment.

ATP = adenosine triphosphate; DON = 6-diazo-5-oxo-l-norleucine; ECAR5 = extracellular acidification rate; iLTS5 = iatrogenic laryngotracheal stenosis; OCR = oxygen consumption rate.

Table I

Patient Characteristics

Enrollment	**N = 7**
Median age (range)	41.4 (23–74)
Sex, male/female n (%)	1 (14) / 6 (86)
Tobacco use n (%)	
Current	1 (14)
Former	3 (43)
Never	3 (43)
Cotton-Meyer grade, n (%)	
1	0 (0)
2	1 (14)
3	6 (86)
4	0 (0)
Tracheotomy, n (%)	
Presented with	2 (28)
Required during biopsy	0 (0)
Etiology, n (%)	
Iatrogenic	7 (100)
Congenital	0 (0)
Medication utilization, n (%)	
Autoimmune/autosuppressant therapy	0 (0)
Oxygen therapy	1 (14)
Inhaled steroid	1 (14)
PPI	1 (14)
Comorbidities, n (%)	
Asthma	3 (43)
Chronic obstructive	1 (14)
Depression	3 (43)
Laryngopharyngeal reflux	1 (14)
Hemiplegia	1 (14)
Hypertension	3 (43)
Obstructive sleep apnea	1 (14)
Solid tumor	1 (14)
Inflammatory tissue disease	0 (0)
Aspiration pneumonia secondary to dysphagia	0 (0)
Months from injury to treatment, average (± SEM)	14.9 (± 4.8)

SEM = standard error of the mean; PPI = proton pump inhibitor.